

# Distance of Hydroxyl Functionality from the Quaternized Center Influence DNA Binding and in Vitro Gene Delivery Efficacies of Cationic Lipids with Hydroxyalkyl Headgroups

Yenugonda Venkata Mahidhar,<sup>†</sup> Mukthavaram Rajesh,<sup>†</sup> Sunkara Sakunthala Madhavendra,<sup>‡</sup> and Arabinda Chaudhuri<sup>\*,†</sup>

Division of Lipid Science and Technology and Electron Microscopy Center, Indian Institute of Chemical Technology, Hyderabad-500 007, India

Received May 6, 2004

In vitro gene delivery efficacies of cationic amphiphiles **1–7** (Scheme 1) were measured by both the reporter gene expression assays in CHO, COS-1, HepG2, and MCF7 cells and by the whole cell histochemical X-gal staining of representative Chinese hamster ovary cells. Our results demonstrated that in vitro gene delivery efficiencies of cationic lipids with hydroxyalkyl headgroups are adversely affected by increased covalent distances between the hydroxyl functionality and the cationic centers. Findings in the DNase I protection experiments and transmission electron microscopic study support the notion that such compromised gene delivery efficacies may originate from poor lipid–DNA binding interactions and significantly increased lipoplex nanosizes.

## Introduction

Safety and efficiency of vehicles for delivering therapeutic genes into body cells are the two most important prerequisites toward ensuring clinical success of gene therapy. Recombinant viral vectors, despite being remarkably efficient in transfecting body cells, suffer from numerous biosafety-related disadvantages including generation of inflammatory and immunogenic responses and production of replication-competent virus through recombination events with host genome.<sup>1–8</sup> Conversely, cationic transfection lipids, because of their least immunogenic nature, robust manufacture, ability to deliver large pieces of DNA, and ease of handling and preparation techniques, are finding increasing uses as the nonviral vectors of choice in delivering genes into body cells.<sup>9–24</sup>

Defining the key architectural elements necessary for imparting enhanced transfection properties to cationic amphiphiles through detailed structure–activity investigations using libraries of new cationic lipids is an intensely pursued area of contemporary research in cationic lipid mediated gene delivery. Ever since the pioneering development<sup>25</sup> of glycerol-backbone-based cationic transfection lipid (*N*-[1-(2,3-dioleoyloxy)propyl])-*N,N,N*-trimethylammonium chloride (DOTMA) in 1987, the design and synthesis of more efficacious cationic amphiphiles have been reported.<sup>9–24</sup> Interestingly, in the molecular architectures of many of these subsequently developed cationic transfection lipids, the glycerol backbone of DOTMA was retained. Towards understanding how mandatory is the presence of the glycerol backbone in the molecular structure of cationic transfection lipids, we have designed and synthesized a series of novel non-glycerol-based cationic amphiphiles

and demonstrated that the in vitro gene transfer efficiencies of some of these non-glycerol-based cationic lipids are superior to that of LipofectAmine, one of the most extensively used commercially available liposomal transfection kits.<sup>27–35</sup>

To probe the influence of the distance between the hydroxyl functionality and the cationic centers in modulating the in vitro gene delivery efficacies of the above-mentioned non-glycerol-based cationic transfection lipids containing hydroxyalkyl headgroups, in the present investigation we have designed and synthesized seven novel structural analogues (lipids **1–7**, Scheme 1) of DOMHAC (*N,N*-di-*n*-octadecyl-*N*-2-hydroxyethyl-*N*-methylammonium chloride), one of our previously designed non-glycerol-based cationic lipids.<sup>35</sup> The relative in vitro gene transfer efficacies of lipids **1–7** were measured by reporter gene expression assays in CHO, COS-1, HepG2, and MCF7 cells as well as by whole cell histochemical X-gal staining of the representative CHO cells. In addition, the lipid–DNA binding interaction profiles for lipids **1–7** were evaluated by DNase I sensitivity assays. Results convincingly demonstrate that both in vitro gene transfer properties and the strength of lipid–DNA binding interactions get adversely affected with the increasing distance between the hydroxyl functionality and the quaternized center of cationic lipids with hydroxyalkyl headgroups. Results of the DNase I protection experiments and transmission electron microscopic study, taken together, support the notion that the poor transfection efficacies of cationic lipids with hydroxyl headgroups separated from the positively charged nitrogen atoms by more than three methylene units may originate from weak lipid–DNA binding interactions and increased lipoplex (lipid–DNA complex) sizes.

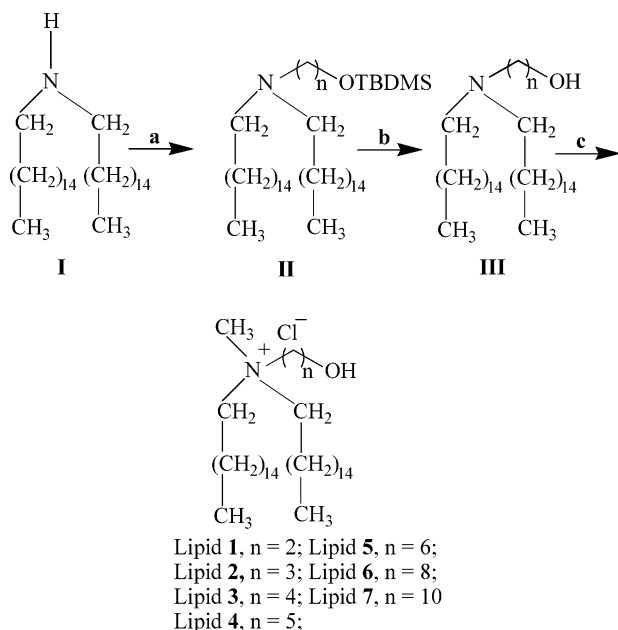
## Results and Discussion

**Chemistry.** Lipids **1–7** (Scheme 1) were synthesized essentially following our previously described method

\* To whom correspondence should be addressed. Phone: 91-40-27193201. Fax: 91-40-27160757. E-mail: arabinda@iict.res.in.

<sup>†</sup> Division of Lipid Science and Technology.

<sup>‡</sup> Electron Microscopy Center.

**Scheme 1.** Synthesis of Lipids 1–7<sup>a</sup>

<sup>a</sup> Reagents: (a) Br-(CH<sub>2</sub>)<sub>n</sub>OTBDMS, K<sub>2</sub>CO<sub>3</sub>, ethyl acetate; (b) TBAF, THF; (c) CH<sub>3</sub>I, DCM, Amberlyst A-26 chloride ion-exchange resin.

for preparing DOMHAC.<sup>35</sup> Briefly, the appropriate *tert*-butyldimethylsilyl-protected bromo alcohols were coupled to *N,N*,di-*n*-hexadecylamine (**I**, Scheme 1) in the presence of potassium carbonate. Tetra-*n*-butylammonium fluoride mediated silyl deprotection of the resulting tertiary amines (**II**, Scheme 1) afforded the tertiary alcohol intermediates (**III**, Scheme 1). Quaternization with excess methyl iodide followed by final ion exchange over Amberlyst A-26 chloride ion-exchange resin afforded the target lipids. Structures of all the final lipids (**1–7**, Scheme 1) were confirmed by <sup>1</sup>H NMR and LSIMS, and the purity of the target lipids were confirmed by C, H, N analysis.

**Transfection Biology.** Figure 1 summarizes the relative efficacies of lipids **1–7** in transfecting CHO, COS-1, HepG2, and MCF7 cells. The cationic liposomes of lipids **1–7** were prepared in combination with equivalent mole of cholesterol as colipid and using pCMV-SPORT-β-gal plasmid as the reporter gene across the lipid/DNA charge ratios of 9:1 to 0.1:1. In general, the transfection efficacies of lipids **1–7** were found to be progressively compromised in all four cells as the distance between the headgroup hydroxyl functionality and the cationic center increased (Figure 1). The most dramatic fall of transfection property was observed with lipid **7** (with 10 methylene units spacer group in its headgroup region), which was found to be practically incompetent in transfecting all the four cells across the entire lipid/DNA charge ratios (Figure 1). The same transfection profiles were further confirmed by whole cell histochemical X-gal staining experiments. Figure 2 shows a representative pattern observed in such whole cell X-gal staining experiments for transfected CHO cells with lipids **1**, **6**, and **7** at a lipid/DNA charge ratio of 1:1. Once again, the transfection efficacies for lipids with long spacer arms between the hydroxyl functionality and the cationic center in the headgroup region (lipids **6** and **7**) were found to be strikingly poor

compared to that of lipid **1** with only two methylene units as the headgroup spacer arm (Figure 2). For the sake of comparison, the transfection profiles of the widely used commercially available DMRIE-C were also included in both the reporter gene expression assay (Figure 1) and the whole cell X-gal staining experiments (Figure 2). Taken together, the results summarized in Figures 1 and 2 convincingly demonstrate that the transfection efficacies of cationic lipids with hydroxy-alkyl headgroups get progressively compromised with increasing distance between the hydroxyl headgroup and the quaternized center.

To gain insight into whether the observed transfection profiles of lipids **1–7** were related to their varying inherent toxicity profiles, MTT-based cell viability assays were performed in representative CHO and COS-1 cells across the entire range of lipid/DNA charge ratios used in the actual transfection experiments. Percent cell viabilities of all the cationic lipids **1–7** were found to be remarkably high even at the higher end of the lipid/DNA ratios (Figure 3). Thus, the cell viability results summarized in Figure 3 ruled out the possibility of inherent cellular cytotoxicities of the individual lipids playing a role behind the observed transfection profiles of lipids **1–7**.

To understand whether the contrasting transfection efficacies of the present cationic lipids could originate from varying lipid/DNA electrostatic binding interactions, we performed the DNase I protection experiments across the entire range of the lipid/DNA charge ratios by monitoring the sensitivities of the lipoplexes upon treatment with DNase I. After the free DNA digestion by DNase I, the total DNA (both digested and inaccessible DNA) was separated from the lipid and DNase I (by extracting with organic solvent) and loaded onto a 1% agarose gel. Figure 4 summarizes the electrophoretic gel patterns observed for representative lipids **1** and **7**. Band intensities of inaccessible and therefore undigested DNA associated with transfection incompetent lipoplexes prepared from lipid **7** were significantly less than those associated with the most transfection efficient lipoplexes made from lipid **1** essentially across the range of lipid/DNA charge ratios of 9:1 to 0.3:1 (Figure 4). Such gel patterns in DNase I sensitivity assays indicate that the plasmid DNA associated with lipid **7** is likely to be more susceptible to degradation by cellular DNase I than the DNA complexed to lipid **1**. Similar gel characteristics in DNase I protection experiments were also observed for lipoplexes prepared with lipid **6** (data not shown). These findings are consistent with the notion that the compromised *in vitro* transfection efficacies of lipids **6** and **7** could, in part, originate from poor lipid–DNA binding interactions, which in turn renders the loosely associated DNA susceptible to degradation by cellular DNase I.

Finally, to find a correlation, if any, between the lipoplex sizes and their *in vitro* gene transfer efficacies, transmission electron microscopic images of the representative lipoplexes prepared from lipids **1**, **4**, and **7** using lipid/DNA charge ratios of 1:1 were taken (Figure 5). Contrastingly, while the aqueous lipoplexes prepared from lipids **1** and **4** were observed to be much smaller and well dispersed, those prepared with lipid **7** were found to be remarkably large and aggregate-forming in

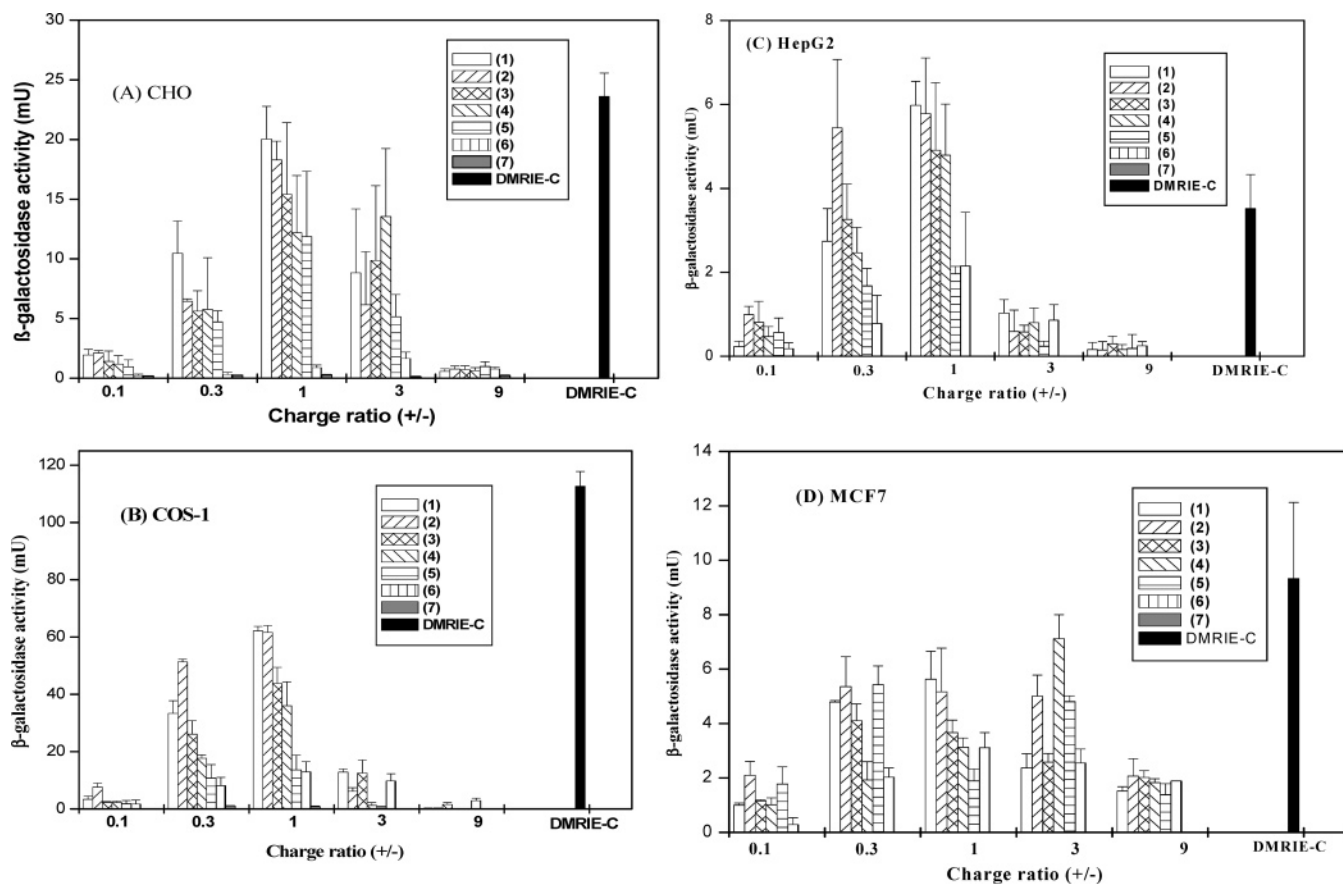


**Figure 1.** In vitro transfection efficiencies of lipids 1–7 in CHO (A), COS-1 (B), and HepG2 (C), and MCF-7 (D) cells using cholesterol as colipid (at lipid/cholesterol mole ratio of 1:1). Units of  $\beta$ -galactosidase activity were plotted against the varying lipid to DNA ( $\pm$ ) charge ratios. The *o*-nitrophenol formation (micromoles of *o*-nitrophenol produced per 10 min) was converted to activity units using a standard curve obtained with pure (commercial)  $\beta$ -galactosidase. The transfection efficiencies of commercially available DMRIE-C are shown for comparison. The transfection values shown are the average of triplicate experiments performed on the same day.

nature (Figure 5). Such relatively big size and aggregate-forming characteristics of the lipoplex prepared with lipid 7 (Figure 5) are likely to play some inhibitory role in the cellular uptake step of the transfection pathway. In addition, we also measured the nanosizes of the pure liposomes (in the presence of DMEM) prepared from cationic lipids 1–7 by the dynamic laser light scattering technique. While the average nanosizes of the liposomes prepared from transfection efficient lipids 1–5 were found to vary within the range 120–170 nm (data not shown), those of liposomes prepared with transfection incompetent lipids 6 and 7 were measured to be  $565 \pm 16$  and  $535 \pm 11$  nm, respectively. Thus, the significantly large sizes might inhibit effective cellular uptake process for liposomes prepared with lipids 6 and 7 imparting thereby severely compromised transfection efficiencies to lipids 6 and 7. Moreover, the presence of 8 and 10 methylene units between the positively charged nitrogen atom and the hydroxyl functionality of lipids 6 and 7 essentially makes them “three-tailed” cationic amphiphiles. This, in turn, may adversely affect the stability of the liposomes prepared with lipids 6 and 7, causing them to form larger lipid/DNA complexes and imparting to them poor DNA binding characteristics. Clearly, further cell biology experiments need to be carried out for more mechanistic insights into the origin of lipid 7 being completely transfection-incompetent.

In summary, the results of the present structure–activity investigation involving the use of seven new structural analogues (1–7) of our previously reported cationic transfection lipid DOMHAC<sup>35</sup> demonstrate that the in vitro gene delivery efficacies of simple twin-chain cationic lipids with hydroxyalkyl headgroups get adversely affected with increasing covalent distance between the hydroxyl functionality and the quaternized center. Results of our DNase I protection experiments and transmission electron microscopic images of representative lipoplexes, taken together, indicate that the severely compromised transfection efficacies of lipid 7 may result from the poor lipid–DNA binding interactions and its relatively large size and aggregate-forming characteristics. In conclusion, caution should be exercised in designing future-generation cationic transfection lipids by covalent grafting of hydroxyalkyl headgroups with the hydroxyl functionality far away from the cationic centers.

## Experimental Section

**General Procedures and Materials.** The high-resolution mass spectrometric (HRMS) experiments were performed on a Micromass AUTOSPEC-M mass spectrometer (Manchester, U.K.) with an OPUS V 3.1X data system. Data were acquired by liquid secondary ion mass spectrometry (LSIMS) using *m*-nitrobenzyl alcohol as the matrix. <sup>1</sup>H NMR spectra were recorded on a Varian FT 200 MHz or AV 300 MHz or Varian Unity 500 MHz. Elemental analyses (C, H, N) were performed

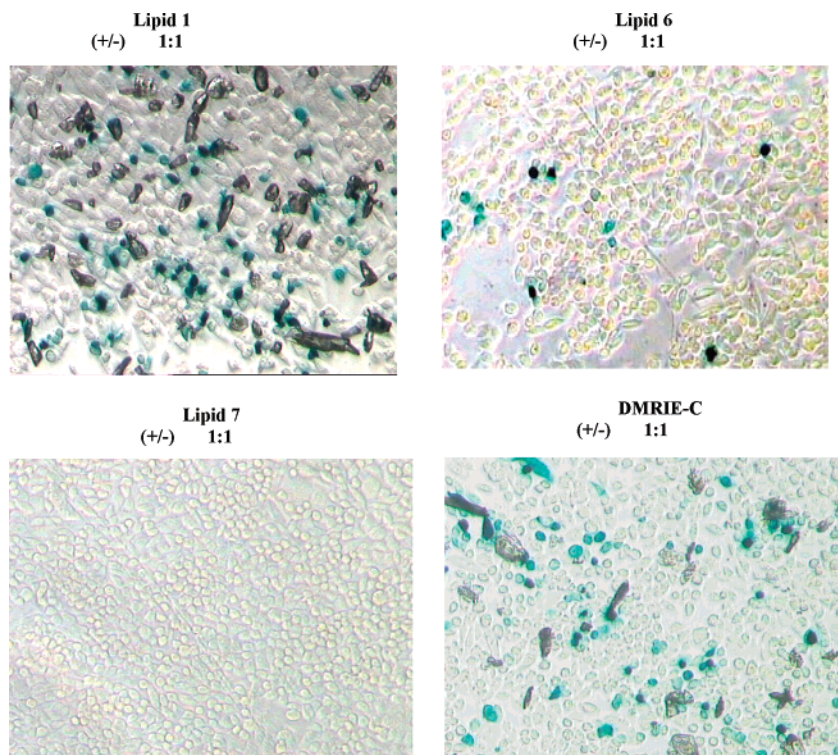


**Figure 2.** Histochemical whole cell X-gal staining of transfected CHO cells with lipids **1**, **6**, and **7** and DMRIE-C at lipid/DNA charge ratios of 1:1. Cells expressing  $\beta$ -galactosidase were stained with X-gal as described in the text.

on a Perkin-Elmer 240c at our microanalytical facility. 1-Bromohexadecane, *n*-hexadecylamine, *tert*-butyldimethylsilyl chloride, tetra-*n*-butylammonium fluoride (1 M solution in THF), and Amberlyst A-26 were purchased from Lancaster (Morecambe, U.K.). Unless otherwise stated, all reagents were purchased from local commercial suppliers and were used without further purification. Column chromatography was performed with silica gel (Acme Synthetic Chemicals, India, 60–120 mesh). The *p*-CMV-SPORT- $\beta$ -gal plasmid used was a generous gift from Dr. Nalam Madhusudhana Rao of Centre for Cellular and Molecular Biology, Hyderabad, India. Cell culture media, fetal bovine serum, 3-(4,5-dimethylthiazol-2-yl)-2,5-diphenyltetrazolium bromide (MTT), poly(ethylene glycol) 8000, *o*-nitrophenyl- $\beta$ -D-galactopyranoside, and cholesterol were purchased from Sigma, St. Louis, MO. NP-40, antibiotics, and agarose were purchased from Hi-media, India. Unless otherwise stated, all reagents were purchased from local commercial suppliers and were used without further purification. COS-1 (SV 40 transformed African green monkey kidney cells), and CHO (Chinese hamster ovary), MCF-7 (human breast adenocarcinoma cell), and HEPG2 (human hepatoblastoma cell) cell lines were procured from the National Centre for Cell Sciences (NCCS), Pune, India. Cells were grown at 37 °C in Dulbecco's modified Eagle's medium (DMEM) with 10% FBS in a humidified atmosphere containing 5% CO<sub>2</sub>/95% air. The purity of lipids **1–7** was confirmed by elemental analyses (C, H, N).

**Syntheses of Lipids 1–7.** As representative details, syntheses and spectral characterization of lipid **1** and all their synthetic intermediates shown in Scheme 1 are provided below. Lipids **2–7** were synthesized following essentially the same protocols adopted for preparing lipid **1**.

**Synthesis of *N,N*-Di-*n*-hexadecyl-*N*-methyl-*N*-(2-hydroxyethyl)ammonium Chloride (Lipid **1**, Scheme 1).** **Step a.** A mixture of *N,N*-di-*n*-hexadecylamine (1.00 g, 2.2 mmol, prepared as described previously<sup>35</sup>) and 2-bromoethyl *tert*-butyldimethylsilyl ether (0.61 g, 2.6 mmol, prepared by reacting 2-bromoethanol and *tert*-butyldimethylsilyl chloride in the presence of imidazole followed by the usual workup) was refluxed in ethyl acetate (25 mL) in the presence of anhydrous potassium carbonate (0.74 g, 5.4 mmol) for 40 h.

The reaction mixture was taken in ethyl acetate (50 mL) and washed with water (2 × 50 mL), dried over anhydrous sodium sulfate, and filtered, and the filtrate was concentrated on a rotary evaporator. The residue upon purification by column chromatography (using 60–120 mesh size silica gel and 2% ethyl acetate in hexane as eluent) afforded the intermediate tertiary amine, namely, *O-tert*-butyldimethylsilyl derivative of *N*-2-hydroxyethyl-*N,N*-di-*n*-hexadecylamine (**II**, Scheme 1) as a semisolid (0.62 g, 46% yield, *R*<sub>f</sub> = 0.6, 10:90 ethyl acetate/hexane). <sup>1</sup>H NMR (200 MHz, CDCl<sub>3</sub>) of intermediate **II** (Scheme 1):  $\delta$  (ppm) = 0.00–0.10 (6H, Si(CH<sub>3</sub>)<sub>2</sub>), 0.90–1.00 (m, 15H, (CH<sub>3</sub>)<sub>3</sub>C–Si(CH<sub>3</sub>)<sub>2</sub>–O– and (CH<sub>3</sub>(CH<sub>2</sub>)<sub>14</sub>)<sub>2</sub>), 1.20–1.60 [m, 56H, –N(–CH<sub>2</sub>–(CH<sub>2</sub>)<sub>14</sub>–CH<sub>3</sub>)<sub>2</sub>], 2.40–2.60 (m, 6H, N(CH<sub>2</sub>)<sub>3</sub>), 3.60 (t, 2H, –CH<sub>2</sub>–O–Si(CH<sub>3</sub>)<sub>2</sub>C(CH<sub>3</sub>)<sub>3</sub>).

**Step b.** Tetrabutylammonium fluoride (1.3 mmol, 0.4 mL of 1.0 M tetrabutylammonium fluoride solution in tetrahydrofuran) was added at 0 °C to a solution of compound **II** (0.40 g, 0.7 mmol) in dry tetrahydrofuran (15 mL), and the reaction mixture was kept under stirring at 0 °C for 2 h. The temperature was then raised to room temperature for 6 h. The reaction mixture was then taken in 50 mL of chloroform and washed with water (3 × 20 mL). The organic layer was separated, dried over anhydrous Na<sub>2</sub>SO<sub>4</sub>, filtered, and concentrated on a rotary evaporator. The residue upon purification by column chromatography (using 60–120 mesh size silica gel and 16% ethyl acetate in hexane as eluent) afforded compound *N*-2-hydroxyethyl-*N,N*-di-*n*-hexadecylamine (**III**, Scheme 1) as a liquid (0.17 g, 50% yield, *R*<sub>f</sub> = 0.4, 30:70 ethyl acetate/hexane). <sup>1</sup>H NMR (200 MHz, CDCl<sub>3</sub>) of intermediate **III** (Scheme 1):  $\delta$  (ppm) = 0.90 (t, 6H, [(CH<sub>3</sub>)–(CH<sub>2</sub>)<sub>14</sub>]<sub>2</sub>), 1.20–1.60 [m, 56H, –N(–CH<sub>2</sub>–(CH<sub>2</sub>)<sub>14</sub>–CH<sub>3</sub>)<sub>2</sub>], 2.40–2.60 (m, 6H, N(CH<sub>2</sub>)<sub>3</sub>), 3.60 (t, 2H, –CH<sub>2</sub>–OH). FABMS (LSIMS), *m/z*: 511 [M]<sup>+</sup> + 2 for C<sub>34</sub>H<sub>71</sub>NO.

**Step c.** Methyl iodide (6 mL) was added to intermediate **III** (prepared in step b, 0.14 g, 0.27 mmol) dissolved in 4 mL of 5:4 chloroform/methanol (v/v), and the reaction mixture was kept at room temperature for 3 h. The reaction mixture was concentrated on a rotary evaporator, and the residue upon purification by column chromatography (using 60–120 silica gel mesh size and 2% methanol in chloroform as eluent) followed by chloride ion exchange (using Amberlyst A-26 with

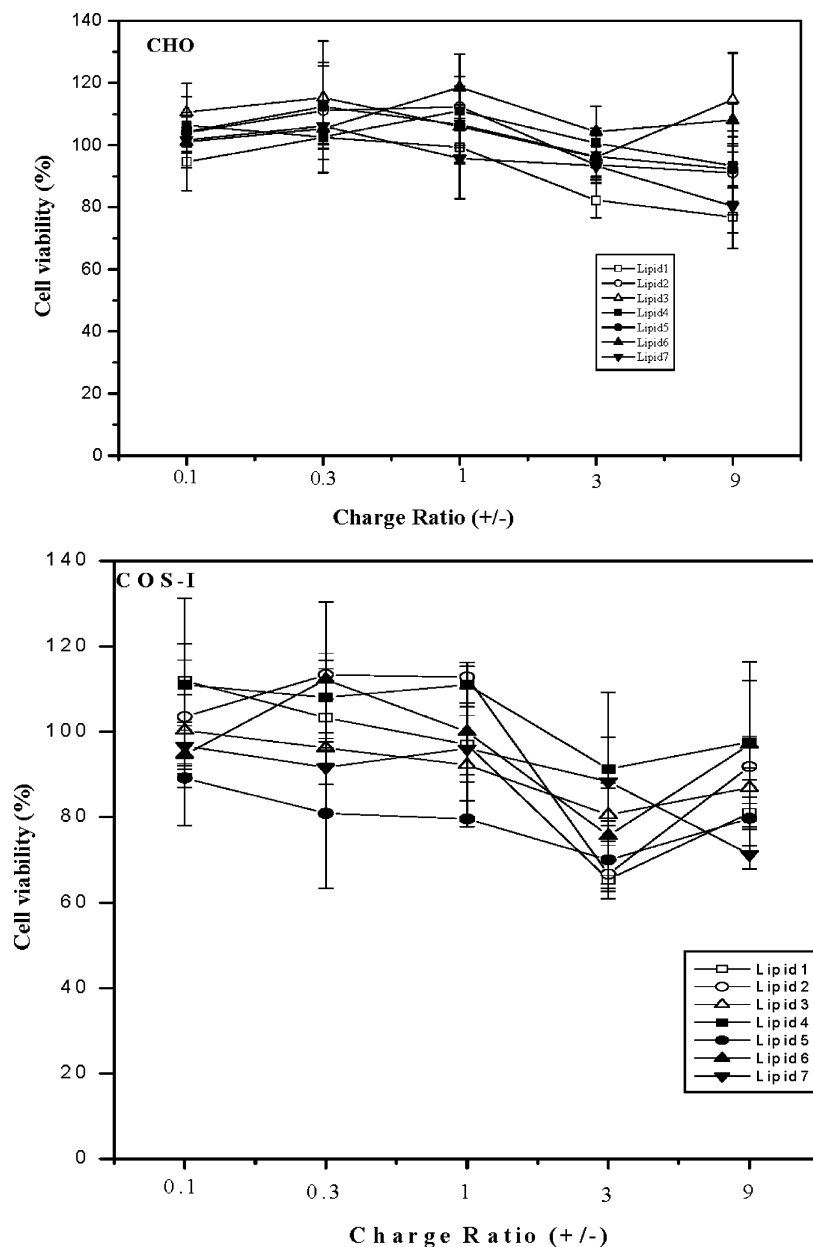


**Figure 3.** MTT-assay-based cellular cytotoxicities of lipids 1–7 against representative CHO and COS-I cells (details of assay protocol are described in the main text). The percent cell viability values shown are the average of triplicate experiments performed on the same day. Results were expressed as percent viability =  $\{[A_{550}(\text{treated cells}) - \text{background}]/[A_{550}(\text{untreated cells}) - \text{background}]\} \times 100$ .

methanol as eluent) afforded the pure title lipid **1** (80 mg, 58% yield, white solid,  $R_f = 0.4$  with 5:95 methanol/chloroform).  $^1\text{H NMR}$  (200 MHz,  $\text{CDCl}_3$ ):  $\delta$  (ppm) = 0.90 (t, 6H,  $[\text{CH}_3(\text{CH}_2)_{15}]_2$ ), 1.20–1.60 [m, 52H,  $-\text{N}(-\text{CH}_2-\text{CH}_2-(\text{CH}_2)_{13}-\text{CH}_3)_2$ ], 1.60–1.80 (brs, 4H,  $\text{CH}_3(\text{HOCH}_2-\text{CH}_2)\text{N}^+[\text{CH}_2-\text{CH}_2-(\text{CH}_2)_{13}-\text{CH}_3]_2$ ), 3.39 [s, 3H,  $\text{CH}_3(\text{HOCH}_2-\text{CH}_2)\text{N}^+$ ], 3.40–3.60 [brs, 4H,  $\text{CH}_3(\text{HOCH}_2-\text{CH}_2)\text{N}^+(-\text{CH}_2-\text{CH}_2-(\text{CH}_2)_{13}-\text{CH}_3)_2$ ], 3.70–3.85 (2H,  $\text{CH}_3(\text{HOCH}_2-\text{CH}_2)\text{N}^+$ ), 4.10–4.30 (m, 3H,  $\text{CH}_3(\text{HOCH}_2-\text{CH}_2)\text{N}^+$ ) and OH). FABMS (LSIMS),  $m/z$ : 525  $[\text{M}]^+ + 1$  for  $\text{C}_{35}\text{H}_{74}\text{NOCl}$ . Anal. ( $\text{C}_{35}\text{H}_{74}\text{NOCl}$ ) C, H, N.

**Synthesis of Lipids 2–7.** Lipids 2–7 (white solids) were synthesized following the same synthetic procedure as described above for preparing lipid **1** except using the appropriate *tert*-butyldimethylsilyl protected bromoalkanols. All the isolated intermediates gave spectroscopic data in agreement with their structures shown in Scheme 1. The  $^1\text{H NMR}$  and LSIMS results for the new lipids 2–7 are provided below.

**Lipid 2 (*N,N*-Di-*n*-hexadecyl-*N*-methyl-*N*-(3-hydroxy-*n*-propyl)ammonium chloride).**  $^1\text{H NMR}$  (300 MHz,  $\text{CDCl}_3$ ):  $\delta$  (ppm) = 0.90 (t, 6H,  $[\text{CH}_3(\text{CH}_2)_{15}]_2$ ), 1.20–1.60 (m, 52H,

$-\text{N}(-\text{CH}_2-\text{CH}_2-(\text{CH}_2)_{13}-\text{CH}_3)_2$ ), 1.60–1.80 (brs, 4H,  $\text{CH}_3(\text{HOCH}_2-\text{CH}_2)\text{N}^+(\text{CH}_2-\text{CH}_2)_2$ ), 2.00–2.20 (brs, 2H,  $\text{CH}_3(\text{HOCH}_2-\text{CH}_2-\text{CH}_2-\text{CH}_2)\text{N}^+$ ), 3.23 [s, 3H,  $\text{CH}_3(\text{HOCH}_2-\text{CH}_2-\text{CH}_2-\text{CH}_2)\text{N}^+(\text{CH}_2-\text{CH}_2)_2$ ], 3.30–3.40 (brs, 4H,  $\text{CH}_3(\text{HOCH}_2-\text{CH}_2-\text{CH}_2-\text{CH}_2)\text{N}^+(\text{CH}_2-\text{CH}_2)_2$ ), 3.70–3.80 (4H,  $\text{CH}_3(\text{HOCH}_2-\text{CH}_2-\text{CH}_2-\text{CH}_2)\text{N}^+$ ), 3.90–4.00 (m, 1H, OH). FABMS (LSIMS),  $m/z$ : 538  $[\text{M}]^+ + 1$  for  $\text{C}_{36}\text{H}_{76}\text{NOCl}$ . Anal. ( $\text{C}_{36}\text{H}_{76}\text{NOCl}$ ) C, H, N.

**Lipid 3 (*N,N*-Di-*n*-hexadecyl-*N*-methyl-*N*-(4-hydroxy-*n*-butyl)ammonium chloride).**  $^1\text{H NMR}$  (200 MHz,  $\text{CDCl}_3$ ):  $\delta$  (ppm) = 0.90 (t, 6H,  $[\text{CH}_3(\text{CH}_2)_{15}]_2$ ), 1.20–1.60 (m, 52H,  $-\text{N}(-\text{CH}_2-\text{CH}_2-(\text{CH}_2)_{13}-\text{CH}_3)_2$ ), 1.60–2.10 (m, 8H,  $\text{CH}_3(\text{HOCH}_2-\text{CH}_2-\text{CH}_2-\text{CH}_2-\text{CH}_2)\text{N}^+(\text{CH}_2-\text{CH}_2)_2$ ), 3.35 (s, 3H,  $\text{CH}_3(\text{HOCH}_2-(\text{CH}_2)_2-\text{CH}_2)\text{N}^+$ ), 3.40–3.80 (m, 8H,  $\text{CH}_3(\text{HOCH}_2-(\text{CH}_2)_2-\text{CH}_2)\text{N}^+(\text{CH}_2-\text{CH}_2)_2$ ). FABMS (LSIMS),  $m/z$ : 553  $[\text{M}]^+ + 1$  for  $\text{C}_{37}\text{H}_{78}\text{NOCl}$ . Anal. ( $\text{C}_{37}\text{H}_{78}\text{NOCl}$ ) C, H, N.

**Lipid 4 (*N,N*-Di-*n*-hexadecyl-*N*-methyl-*N*-(5-hydroxy-*n*-pentyl)ammonium chloride).**  $^1\text{H NMR}$  (200 MHz,  $\text{CDCl}_3$ ):  $\delta$  (ppm) = 0.90 (t, 6H,  $[\text{CH}_3(\text{CH}_2)_{15}]_2$ ), 1.20–1.98 (m, 62H,  $(\text{HOCH}_2-(\text{CH}_2)_3-\text{CH}_2)\text{N}^+(-\text{CH}_2-(\text{CH}_2)_{14}-\text{CH}_3)_2$ ), 3.30 (s, 3H,  $\text{CH}_3(\text{HOCH}_2-(\text{CH}_2)_3-\text{CH}_2)\text{N}^+$ ), 3.35–3.70 (m, 8H,  $\text{CH}_3$

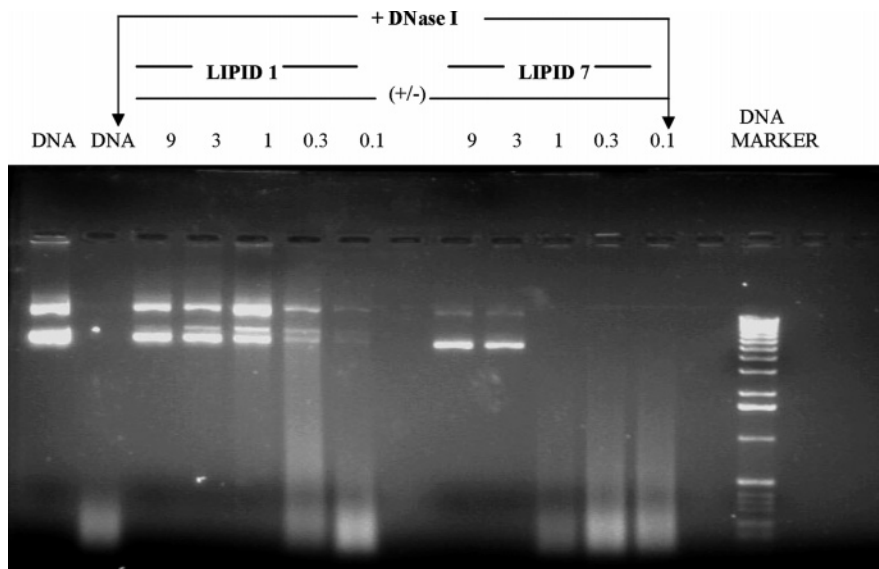


**Figure 4.** DNase I sensitivities of lipid/DNA complexes made from the representative cationic lipids **1** and **7** and pCMV-SPORT- $\beta$ -gal. Free pCMV-SPORT- $\beta$ -gal and pCMV-SPORT- $\beta$ -gal treated with DNase I were loaded in lanes 1 and 2 from the left, respectively. DNase I treated lipoplexes of lipids **1** and **7** at the indicated lipid/DNA charge ratios were loaded in the next 10 lanes from the left, and the DNA markers were loaded in the extreme right lane. The details of the treatment are as described in the text.

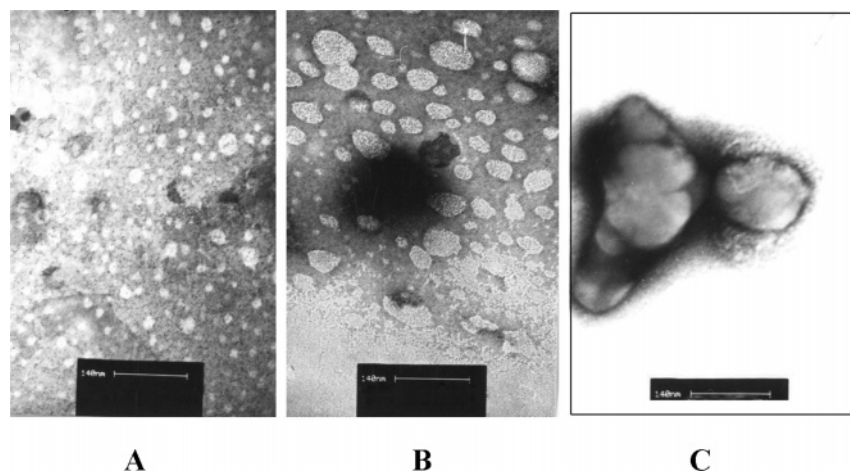


**Figure 5.** Transmission electron micrographs of representative lipoplexes prepared from pCMV-SPORT- $\beta$ -gal and the representative cationic lipids **1** (A), **4** (B), and **7** (C) at a lipid/DNA charge ratio of 1:1. Bars in parts A–C correspond to 140 nm. Experimental details are as described in the text.

(HOCH<sub>2</sub>-(CH<sub>2</sub>)<sub>3</sub>-CH<sub>2</sub>)N<sup>+</sup>(CH<sub>2</sub>-CH<sub>2</sub>)<sub>2</sub>). FABMS (LSIMS), *m/z*: 567 [M]<sup>+</sup> + 1 for C<sub>38</sub>H<sub>80</sub>NOCl. Anal. (C<sub>38</sub>H<sub>80</sub>NOCl) C, H, N.

**Lipid 5** (*N,N*-Di-*n*-hexadecyl-*N*-methyl-*N*-(6-hydroxy-*n*-hexyl)ammonium chloride). <sup>1</sup>H NMR (300 MHz, CDCl<sub>3</sub>):  $\delta$  (ppm) = 0.90 (t, 6H, [CH<sub>3</sub>(CH<sub>2</sub>)<sub>15</sub>]<sub>2</sub>), 1.20–1.98 (m, 64H, (HOCH<sub>2</sub>-(CH<sub>2</sub>)<sub>4</sub>-CH<sub>2</sub>)N-(CH<sub>2</sub>-(CH<sub>2</sub>)<sub>14</sub>-CH<sub>3</sub>)<sub>2</sub>), 3.35 (s, 3H, CH<sub>3</sub>(HOCH<sub>2</sub>-(CH<sub>2</sub>)<sub>4</sub>-CH<sub>2</sub>)N<sup>+</sup>), 3.40–3.70 (m, 8H, CH<sub>3</sub>-(HOCH<sub>2</sub>-(CH<sub>2</sub>)<sub>4</sub>-CH<sub>2</sub>)N<sup>+</sup>(CH<sub>2</sub>-CH<sub>2</sub>)<sub>2</sub>). FABMS (LSIMS), *m/z*: 581 [M]<sup>+</sup> + 1 for C<sub>39</sub>H<sub>82</sub>NOCl. Anal. (C<sub>39</sub>H<sub>82</sub>NOCl) C, H, N.

**Lipid 6** (*N,N*-Di-*n*-hexadecyl-*N*-methyl-*N*-(8-hydroxy-*n*-octyl)ammonium chloride). <sup>1</sup>H NMR (200 MHz, CDCl<sub>3</sub>):  $\delta$  (ppm) = 0.90 (t, 6H, [CH<sub>3</sub>(CH<sub>2</sub>)<sub>15</sub>]<sub>2</sub>), 1.10–2.00 (m, 68H, (HOCH<sub>2</sub>-(CH<sub>2</sub>)<sub>6</sub>-CH<sub>2</sub>)N-(CH<sub>2</sub>-(CH<sub>2</sub>)<sub>14</sub>-CH<sub>3</sub>)<sub>2</sub>), 3.35 (s, 3H, CH<sub>3</sub>(HOCH<sub>2</sub>-(CH<sub>2</sub>)<sub>6</sub>-CH<sub>2</sub>)N<sup>+</sup>), 3.40–3.70 (m, 8H, CH<sub>3</sub>-(HOCH<sub>2</sub>-(CH<sub>2</sub>)<sub>6</sub>-CH<sub>2</sub>)N<sup>+</sup>(CH<sub>2</sub>-CH<sub>2</sub>)<sub>2</sub>). FABMS (LSIMS), *m/z*: 609 [M]<sup>+</sup> + 1 for C<sub>41</sub>H<sub>86</sub>NOCl. Anal. (C<sub>41</sub>H<sub>86</sub>NOCl) C, H, N.

**Lipid 7** (*N,N*-Di-*n*-hexadecyl-*N*-methyl-*N*-(10-hydroxy-*n*-dodecyl)ammonium chloride). <sup>1</sup>H NMR (200 MHz, CDCl<sub>3</sub>):  $\delta$  (ppm) = 0.90 (t, 6H, [CH<sub>3</sub>(CH<sub>2</sub>)<sub>15</sub>]<sub>2</sub>), 1.20–1.80 (m, 72H, (HOCH<sub>2</sub>-(CH<sub>2</sub>)<sub>8</sub>-CH<sub>2</sub>)N-(CH<sub>2</sub>-(CH<sub>2</sub>)<sub>14</sub>-CH<sub>3</sub>)<sub>2</sub>), 3.20 (s, 3H, CH<sub>3</sub>(HOCH<sub>2</sub>-(CH<sub>2</sub>)<sub>8</sub>-CH<sub>2</sub>)N<sup>+</sup>(CH<sub>2</sub>-CH<sub>2</sub>)<sub>2</sub>), 3.20–3.70 (m, 8H, CH<sub>3</sub>(HOCH<sub>2</sub>-(CH<sub>2</sub>)<sub>8</sub>-CH<sub>2</sub>)N<sup>+</sup>(CH<sub>2</sub>-CH<sub>2</sub>)<sub>2</sub>). FABMS

(LSIMS), *m/z*: 637 [M]<sup>+</sup> + 1 for C<sub>43</sub>H<sub>90</sub>NOCl. Anal. (C<sub>43</sub>H<sub>90</sub>NOCl) C, H, N.

**Preparation of Liposomes.** The cationic lipid and cholesterol in 1:1 mole ratio were dissolved in a mixture of chloroform and methanol (3:1, v/v) in a glass vial. The solvent was removed with a thin flow of moisture-free nitrogen gas, and the dried lipid film was then kept under high vacuum for 8 h. An amount of 5 mL of sterile deionized water was added to the vacuum-dried lipid film, and the mixture was allowed to swell overnight. The vial was then vortexed for 2–3 min at room temperature to produce multilamellar vesicles (MLVs). MLVs were then sonicated in an ice bath until clarity was attained using a Branson 450 sonifier at 100% duty cycle and 25 W output power to produce small unilamellar vesicles (SUVs).

**Preparation of Plasmid DNA.** pCMV-SPORT- $\beta$ -gal plasmid DNA was prepared by alkaline lysis procedure and purified by PEG-8000 precipitation according to the protocol described by Maniatis and co-workers.<sup>36</sup> The plasmid preparations showing a value of OD<sub>260</sub>/OD<sub>280</sub> more than 1.8 were used.

**Transfection Biology.** Cells were seeded at a density of 20 000 cells (for CHO, MCF-7, HepG2) and 15 000 cells (for

COS-1) per well in a 96-well plate 18–24 h before the transfection. An amount of 0.3  $\mu\text{g}$  of plasmid DNA was complexed with varying amounts of lipids (0.09–8.1 nmol) in plain DMEM medium (total volume made up to 100  $\mu\text{L}$ ) for 30 min. The lipid/DNA charge ratios were varied from 0.1:1 to 9:1 over these ranges of the lipids. The complexes were then added to the cells. After 3 h of incubation, 100  $\mu\text{L}$  of DMEM with 20% FBS was added to the cells. The medium was changed to 10% complete medium after 24 h, and the reporter gene activity was estimated after 48 h. The cells were washed twice with PBS (100  $\mu\text{L}$  each) and lysed in 50  $\mu\text{L}$  of lysis buffer [0.25 M Tris-HCl, pH 8.0, 0.5% NP40]. Care was taken to ensure complete lysis. The  $\beta$ -galactosidase activity per well was estimated by adding 50  $\mu\text{L}$  of 2 $\times$  substrate solution [1.33 mg/mL of ONPG, 0.2 M sodium phosphate (pH 7.3), and 2 mM magnesium chloride] to the lysate in a 96-well plate. Absorption at 405 nm was converted to  $\beta$ -galactosidase units by use of a calibration curve constructed with pure commercial  $\beta$ -galactosidase enzyme. The values of  $\beta$ -galactosidase units in triplicate experiments assayed on the same day varied by less than 20%. The transfection efficiency values shown in Figure 1 are the average of triplicate experiments performed on the same day. Each transfection experiment was repeated twice, and the day-to-day variation in average transfection efficiency was found to be within 2-fold. The transfection profiles obtained on different days were identical.

**Toxicity Assay.** Cytotoxicities of the lipids 1–7 were assessed by the 3-(4,5-dimethylthiazol-2-yl)-2,5-diphenyltetrazolium bromide (MTT) reduction assay as described earlier.<sup>27</sup> The cytotoxicity assay was performed in 96-well plates by maintaining the same ratio of number of cells to amount of cationic lipid, as used in the transfection experiments. MTT was added 3 h after addition of cationic lipid to the cells. Results were expressed as percent viability =  $\{[A_{540}(\text{treated cells}) - \text{background}] / [A_{540}(\text{untreated cells}) - \text{background}]\} \times 100$ .

**DNase I Sensitivity Assay.** Briefly, in a typical assay pCMV- $\beta$ -gal (1000 ng) was complexed with the varying amount of cationic lipids (using indicated lipid/DNA charge ratios in Figure 4) in a total volume of 30  $\mu\text{L}$  in Hepes buffer, pH 7.40, and incubated at room temperature for 30 min on a rotary shaker. Subsequently, the complexes were treated with 10  $\mu\text{L}$  of DNase I (at a final concentration of 1  $\mu\text{g}/\text{mL}$ ) in the presence of 20 mM  $\text{MgCl}_2$  and incubated for 20 min at 37  $^\circ\text{C}$ . The reactions were then halted by adding EDTA (to a final concentration of 50 mM) and incubation of the mixture at 60  $^\circ\text{C}$  for 10 min in a water bath. The aqueous layer was washed with 50  $\mu\text{L}$  of phenol/chloroform/isoamyl alcohol (25:24:1 mixture, v/v/v) and centrifuged at 10000g for 5 min. The aqueous supernatants were separated, loaded (15  $\mu\text{L}$ ) on a 1% agarose gel (prestained with ethidium bromide), and electrophoresed at 100 V for 1 h.

**X-Gal Staining.** Cells expressing  $\beta$ -galactosidase were histochemically stained with the substrate 5-bromo-4-chloro-3-indolyl- $\beta$ -D-galactopyranoside (X-gal) as described previously.<sup>29</sup> Briefly, 48 h after transfection with lipoplexes in 96-well plates, the cells were washed two times (2  $\times$  100  $\mu\text{L}$ ) with phosphate-buffered saline (PBS, 137 mM NaCl, 2.7 mM KCl, 10 mM  $\text{Na}_2\text{HPO}_4$ , 2 mM  $\text{KH}_2\text{PO}_4$ , pH 7.4) and fixed with 0.5% glutaraldehyde in PBS (225  $\mu\text{L}$ ). After 15 min of incubation at room temperature, the cells were washed again with PBS three times (3  $\times$  250  $\mu\text{L}$ ) and subsequently were stained with 1.0 mg/mL X-gal in PBS containing 5.0 mM  $\text{K}_3[\text{Fe}(\text{CN})_6]$  and 5.0 mM  $\text{K}_4[\text{Fe}(\text{CN})_6]$  and 1 mM  $\text{MgSO}_4$  for 2–4 h at 37  $^\circ\text{C}$ . Blue cells were identified by light microscope (Leica, Germany).

**Transmission Electron Microscopy.** Electron microscopy was performed on an FEI Tecnai 12 TEM apparatus operated at 100 kV. Lipoplex samples were transferred onto an ultrathin carbon-coated copper grid by placing the grid on top of a 10  $\mu\text{L}$  drop of the sample for 1 min. After the excess fluid from one side was wicked away, the grid was placed on a 100  $\mu\text{L}$  water drop for a 30 s wash. The excess fluid was removed, and the grid was placed for 1 min on a 20  $\mu\text{L}$  drop of freshly

filtered uranyl acetate (1.33%). Once again, the excess fluid was wicked away and the grid was air-dried.

**Acknowledgment.** Financial support received from the Department of Biotechnology, Government of India (to A.C.) is gratefully acknowledged. Y.V.M. and M.R. thank the Council of Scientific and Industrial Research (CSIR), Government of India, for their doctoral research fellowship.

**Supporting Information Available:** Elemental analysis results (C, H, N) for lipids 1–7. This material is available free of charge via the Internet at <http://pubs.acs.org>.

## References

- (1) Verma, I. M.; Somina, M. Gene Therapy—Promises, Problems and Prospects. *Nature* **1997**, *389*, 239–242.
- (2) Anderson, W. F. Human Gene Therapy. *Nature* **1998**, *392*, 25–30.
- (3) Yla-Herttuala, S.; Martin, J. F. Cardiovascular Gene Therapy. *Lancet* **2000**, *355*, 213–222.
- (4) Yang, Y.; Nunes, F. A.; Berencsi, K.; Furth, E. E.; Gonczol, E.; Wilson, J. M. Cellular Immunity to Viral Antigens Limits E1-Deleted Adenoviruses for Gene Therapy. *Proc. Natl. Acad. Sci. U.S.A.* **1994**, *91*, 4407–4411.
- (5) Knowles, M. R.; Hohnaker, K. W.; Zhou, Z.; Olsen, J. C.; Noah, T. L.; Hu, P. C.; Leigh, M. W.; Engelhardt, J. F.; Edwards, L. J.; Jones, K. R.; Boucher, R. A. Controlled Study of Adenoviral-Vector Mediated Gene Transfer in the Nasal Epithelium of Patients with Cystic Fibrosis. *N. Engl. J. Med.* **1995**, *333*, 823–831.
- (6) Crystal, R. G.; McElvaney, N. G.; Rosenfeld, M. A.; Chu, C. S.; Mastrangeli, A.; Hay, J. G.; Brody, S. L.; Jaffe, H. A.; Eissa, N. T.; Danel, C. Administration of an Adenovirus Containing the Human CFTR cDNA to the Respiratory Tract of Individuals with Cystic Fibrosis. *Nat. Genet.* **1994**, *8*, 42–51.
- (7) Yang, Y.; Nunes, F. A.; Berencsi, K.; Gonczol, E.; Engelhardt, J. F.; Wilson, J. Inactivation of E2a in Recombinant Adenoviruses Improves the Prospect for Gene Therapy in Cystic Fibrosis. *Nat. Genet.* **1994**, *7*, 362–369.
- (8) Lehrman, S. Virus Treatment Questioned after Gene Therapy Death. *Nature* **1999**, *401*, 517–518.
- (9) Fabio, K.; Gaucheron, J.; Giorgio, C. D.; Vierling, P. Novel Galactosylated Polyamine Bolaamphiphiles for Gene Delivery. *Bioconjugate Chem.* **2003**, *14*, 358–367.
- (10) Heyes, J. A.; Duvaz, D. N.; Cooper, R. G.; Springer, C. J. Synthesis of Novel Cationic Lipids: Effect of Structural Modification on the Efficiency of Gene Transfer. *J. Med. Chem.* **2002**, *45*, 99–114.
- (11) McGregor, C.; Perrin, C.; Monck, M.; Camilleri, P.; Kirby, A. J. Rational Approaches to the Design of Cationic Gemini Surfactants for Gene Delivery. *J. Am. Chem. Soc.* **2001**, *123*, 6215–6220.
- (12) Guenin, E.; Herve, A. C.; Floch, V.; Loisel, S.; Yaounac, J. J.; Clement, J. C.; Ferec, C.; des Abbayes, H. Cationic Phosphonolipids Containing Quaternary Phosphonium and Arsonium Groups for DNA Transfection with Good Efficiency and Low Cellular Toxicity. *Angew. Chem., Int. Ed.* **2000**, *39*, 629–631.
- (13) Floch, V.; Loisel, S.; Guenin, E.; Herve, A. C.; Clement, J. C.; Yaouanc, J. J.; des Abbayes, H.; Ferec, C. Cation Substitution in Cationic Phosphono Lipids: A New Concept To Improve Transfection Activity and Decrease Cellular Toxicity. *J. Med. Chem.* **2000**, *43*, 4617–4628.
- (14) Ghosh, Y. K.; Visweswariah, S. S.; Bhattacharya, S. Nature of Linkage between the Cationic Headgroup and Cholesterol Skeleton Controls Gene Transfection Efficiency. *FEBS Lett.* **2000**, *473*, 341–344.
- (15) Fichert, T.; Regelin, A.; Massing, U. Synthesis and Transfection Properties of Novel Nontoxic Monocationic Lipids: Variations of Lipid Anchor, Spacer and Headgroup Structure. *Bioorg. Med. Chem. Lett.* **2000**, *10*, 787–791.
- (16) Kawakami, S.; Sato, A.; Nishikawa, M.; Yamashita, F.; Hashida, M. Mannose Receptor Mediated Gene Transfer into Macrophages Using Novel Mannosylated Cationic Liposomes. *Gene Ther.* **2000**, *7*, 292–299.
- (17) Choi, J. S.; Lee, E. J.; Jang, H. S.; Sang, J. P. New Cationic Liposomes for Gene Transfer into Mammalian Cells with High Efficiency and Low Toxicity. *Bioconjugate Chem.* **2000**, *12*, 108–113.
- (18) Byk, G.; Wetzer, B.; Frederic, M.; Dubertret, C.; Pitard, B.; Jaslin, G.; Scherman, D. Reduction-Sensitive Lipopolyamines as a Novel Nonviral Gene Delivery System for Modulated Release of DNA with Improved Transgene Expression. *J. Med. Chem.* **2000**, *43*, 4377–4387.

- (19) Miller, A. D. Cationic Liposomes in Gene Therapy. *Angew. Chem., Int. Ed.* **1998**, *37*, 1768–1785 and references therein.
- (20) Wang, J.; Guo, X.; Xu, Y.; Barron, L.; Szoka, F. C., Jr. Synthesis and Characterization of Long Chain Alkyl Acyl Carnitine Esters. Potentially Biodegradable Cationic Lipids for Use in Gene Delivery. *J. Med. Chem.* **1998**, *41*, 2207–2215.
- (21) Byk, G.; Dubertret, C.; Escriou, V.; Frederic, M.; Jaslin, G.; Rangara, R.; Pitard, B.; Crouzet, J.; Wils, P.; Schwartz, B.; Scherman, D. Synthesis, Activity, and Structure–Activity Relationship Studies of Novel Cationic Lipids for DNA Transfer. *J. Med. Chem.* **1998**, *41*, 224–235.
- (22) Kawakami, S.; Nishikawa, M.; Yamashita, F.; Takakura, Y.; Hashida, M. Asialo Glycoprotein Receptor-Mediated Gene Transfer Using Novel Galactosylated Cationic Liposomes. *Biochem. Biophys. Res. Commun.* **1998**, *252*, 78–83.
- (23) Eastman, S. J.; Siegel, C.; Tousignant, J.; Smith, A. E.; Cheng, S. H.; Scheule, R. K. Biophysical Characterisation of Cationic Lipid:DNA Complexes. *Biochim. Biophys. Acta* **1997**, *1325*, 41–62.
- (24) Felgner, J. H.; Kumar, R.; Sridhar, C. N.; Wheeler, C. J.; Tsai, Y. J.; Border, R.; Ramsey, P.; Martin, M.; Felgner, P. L. Enhanced Gene Delivery and Mechanism Studies with a Novel Series of Cationic Lipid Formulations. *J. Biol. Chem.* **1994**, *269*, 2550–2561.
- (25) Felgner, P. L.; Gadek, T. R.; Holm, M.; Roman, R.; Chan, H. W.; Wenz, M.; Northrop, J. P.; Ringold, G. M.; Danielsen, M. Lipofection: A Highly Efficient Lipid Mediated DNA Transfection Procedure. *Proc. Natl. Acad. Sci. U.S.A.* **1987**, *84*, 7413–7417.
- (26) Niculescu-Duvaz, D.; Heyes, J.; Springer, C. J. Structure–Activity Relationship in Cationic Lipid Mediated Gene Transfection. *Curr. Med. Chem.* **2003**, *10*, 1233–1264 and references therein.
- (27) Karmali, P. P.; Kumar, V. V.; Chaudhuri, A. Design, Syntheses and in Vitro Gene Delivery Efficacies of Novel Mono-, Di-, and Tri-lysinated Cationic Lipids: A Structure Activity Investigation. *J. Med. Chem.* **2004**, *47*, 2123–2132.
- (28) Majeti, B. K.; Singh, R. S.; Yadav, S. K.; Reddy, B. S.; Ramakrishna, S.; Diwan, P. V.; Madhavendra, S. S.; Chaudhuri, A. First Examples of Enhanced Intravenous Transgene Expression in Mouse Lung Using Cyclic-Head Cationic Lipids. *Chem. Biol.* **2004**, *11*, 427–437.
- (29) Singh, R. S.; Chaudhuri, A. Single Additional Methylene Group in the Head-group Region Imparts High Gene Transfer Efficacy to a Transfection-Incompetent Cationic Lipid. *FEBS Lett.* **2004**, *556*, 86–90.
- (30) Kumar, V. V.; Pichon, C.; Refregiers, M.; Guerin, B.; Midoux, P.; Chaudhuri, A. Single Histidine Residue in Head-group Region Is Sufficient To Impart Remarkable Gene Transfection Properties to Cationic Lipids: Evidence for Histidine-Mediated Membrane Fusion at Acidic pH. *Gene Ther.* **2003**, *10*, 1206–1215.
- (31) Kumar, V. V.; Singh, R. S.; Chaudhuri, A. Cationic Transfection Lipids in Gene Therapy: Successes, Set-Backs, Challenges and Promises. *Curr. Med. Chem.* **2003**, *10*, 1297–1306 and references therein.
- (32) Singh, R. S.; Mukherjee, K.; Banerjee, R.; Chaudhuri, A.; Hait, S. K.; Moulik, S.; Ramadas, Y.; Vijayalakshmi, A.; Rao, N. M. Anchor-dependency for Non-Glycerol Based Cationic Lipofectins: Mixed Bag of Regular and Anomalous Transfection Profiles. *Chem.—Eur. J.* **2002**, *8*, 900–909.
- (33) Srilakshmi, G. V.; Sen, J.; Chaudhuri, A.; Ramdas, Y.; Rao, N. M. Anchor-Dependent Lipofection with Non-Glycerol Based Cytofectins Containing Single 2-Hydroxyethyl Head Groups. *Biochim. Biophys. Acta* **2002**, *1559*, 87–95.
- (34) Banerjee, R.; Mahidhar, Y. V.; Chaudhuri, A.; Gopal, V.; Rao, N. M. Design, Synthesis and Transfection Biology of Novel Cationic Glycolipids for Use in Liposomal Gene Delivery. *J. Med. Chem.* **2001**, *44*, 4176–4185.
- (35) Banerjee, R.; Das, P. K.; Srilakshmi, G. V.; Chaudhuri, A.; Rao, N. M. A Novel Series of Non-Glycerol Based Cationic Transfection Lipids for Use in Liposomal Gene Delivery. *J. Med. Chem.* **1999**, *42*, 4292–4299.
- (36) Sambrook, J.; Fritsch, E. F.; Maniatis, T. *Molecular Cloning, A Laboratory Manual*, 2nd ed.; Cold Spring Harbor Laboratory Press: Cold Spring Harbor, NY, 1989.

JM049656J